$Ag/TiO_2/WO_3$ nanoparticles with efficient visible light photocatalytic activity*

LI Yujie[1], HAI Guangyuan[2], DING Guilin[1], WANG Keyan[3], and ZHANG Dequan[3]**

1. Physical Department, Tianjin Ren'ai College, Tianjin 301636, China

2. School of Material Science and Engineering, Tiangong University, Tianjin 300387, China

3. Tianjin SYP Engineering Glass Company, Tianjin 300409, China

(Received 10 May 2021; Revised 10 July 2021)

A simple strategy for synthesizing Ag decorated TiO_2/WO_3 composite nanoparticles by sol-gel method used as recyclable photocatalyst is introduced. The photocatalytic efficiency to the degradation of methyl blue (MB) by $Ag/TiO_2/WO_3$ nanoparticles is studied under ultraviolet-visible (UV-Vis) light irradiation. It shows that the photocatalytic efficiency of $Ag/TiO_2/WO_3$ photocatalyst achieves 96% in 20 min, which is 16 times higher than that of pristine TiO_2 at the same conditions. The $Ag/TiO_2/WO_3$ photocatalyst can still reach the degradation rate of 90% in the fifth degradation experiment, indicating a good stability and photocatalytic activity.

Document code: A **Article ID:** 1673-1905(2022)01-0001-5

DOI https://doi.org/10.1007/s11801-022-1077-y

Water resource pollution and energy shortage are the urgent problems for human beings. Traditional sewage treatment methods including physical adsorption[1], biodegradation[2], chemical precipitation[3] are limited in applications. Since FUJISHIMA et al[4] first discovered TiO_2 photocatalysis of water under ultraviolet (UV) light in 1972, photocatalyst based on semiconductor has been extensively investigated. However, most of photocatalyst can only use 5% energy of the sunlight, resulting in poor photocatalytic efficiency. The visible light is more than 40% of solar energy, so it is important to develop more efficient photocatalyst for visible light.

TiO_2 as a kind of wide gap material (3.2 eV) is widely used in functional ceramics, catalysts, cosmetics, photosensitive materials and white inorganic pigments[5-9]. However, TiO_2 photocatalyst has some deficiencies in applications, such as low utilization rate of light energy and easy electron-hole recombination, resulting in low photocatalytic efficiency. In order to solve the problems, structure modification[10], heterojunction construction[11] and noble metal modification[12] are good strategies for photocatalysts. For example, WANG et al[13] fabricated N-doped TiO_2 structrues which exhibited high visible light catalytic activity. CHEN et al[14] have prepared TiO_2/NiO hierarchical nanostructures whose photocatalytic activity shows 10 times higher than that of pure TiO_2. YAO et al[15] reported $Au/SiO_2@TiO_2$ core-shell microspheres for enhanced photocatalysis activity for the degradation of methyl orange.

In this work, we proposed a simple sol-gel method of preparing $Ag/TiO_2/WO_3$ composite nanoparticles and subsequently examined by scanning electron microscope (SEM), energy dispersive X-ray (EDX), X-ray diffraction (XRD) and electrochemical impedance spectroscopy (EIS) analysis. The photocatalytic properties of TiO_2, TiO_2/WO_3 and $Ag/TiO_2/WO_3$ are investigated by degradation of methyl blue (MB) under UV-visible (UV-Vis) light. Compared with TiO_2/WO_3 and TiO_2 nanaoparticles, the as-prepared $Ag/TiO_2/WO_3$ composite nanaoparticles show improved photocatalytic performance.

In a typical procedure, 11 mL tetramethyl titanate (TBOT) was added to 30 mL ethanol and stirred for 20 min, then 10 mL deionized water and 10 mL glacial acetic acid were added to 10 mL ethanol to obtain yellow solution A. 2.5 g ammonium metatransstate (AMT) and 0.02 g $AgNO_3$ were thoroughly stirred and a proper amount of nitric acid was added to adjust the pH value to 2 to obtain solution B. Subsequently, the solution A and solution B were stirred into mixture and then stood for 24 h to obtain the sol. After that, the sol was dried in a drying oven at 80 ℃ for 24 h. Then, the collected samples were calcined in a furnace at 550 ℃ with a heating rate of 2 ℃/min for 4 h in air. Finally, the calcined products were finely grinded to obtain $Ag/TiO_2/WO_3$ nanoparticles. The fabrication process of TiO_2/WO_3 and TiO_2 samples was similar to that of $Ag/TiO_2/WO_3$ except for the addition of $AgNO_3$ and

* This work has been supported by the Natural Science Foundation of Tianjin (No.20JCZDJC00060).

** E-mail: liyujie_111@126.com

$AgNO_3$/AMT, respectively.

The photocatalytic degradation of the prepared samples was tested by taking MB as the degradation substance under the UV-Vis light. First, the MB solution with a concentration of 300 mg/L was prepared. 300 mL of the prepared MB solution was placed in a 500 mL beaker. The as-prepared samples were added to the beaker with 0.3 g and continuous stirred in the darkroom for 60 min. The mixture was exposed to UV-Vis light, and 5 mL sample solution was taken out every 20 min for centrifugal drying treatment. The content of MB was determined by using UV-Vis spectrophotometer to measure the change of the visible light absorption of centrifugal drying MB to the wavelength of 664 nm. The degradation rate of MB was calculated using the following equation

$$MB_{\text{removal}} = (C_0 - C) / C_0, \quad (1)$$

where C_0 is the absorbance of the initial concentration of MB solution and C is the absorbance of the MB solution.

The morphology of as-prepared photocatalysts is characterized by SEM, as shown in Fig.1. As can be observed, the morphologies of all samples prepared by sol-gel method are nanoparticles. Fig.1(a) and (b) show that the particles are of 100—400 nm in size. The $Ag/TiO_2/WO_3$ samples with well dispersion are of 50—100 nm in particle size (Fig.1(c)). The energy dispersive spectrometer (EDS) results of $Ag/TiO_2/WO_3$ samples reveal that Ti, W, O and Ag are detected in the samples with no other impurity elements (Fig.1(d)). The tiny particles with large surface areas will provide more active sites to facilitate photocatalytic reactions.

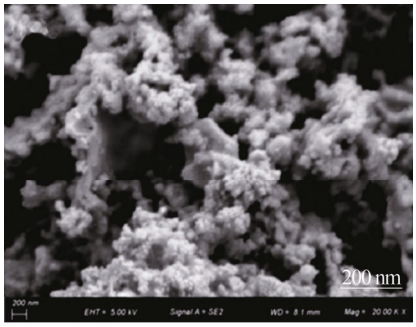

(a)

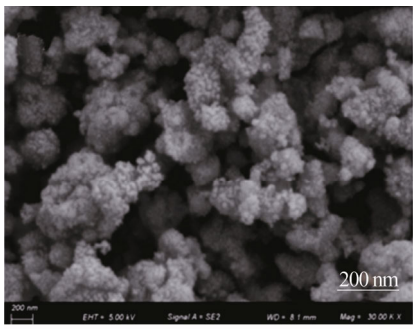

(b)

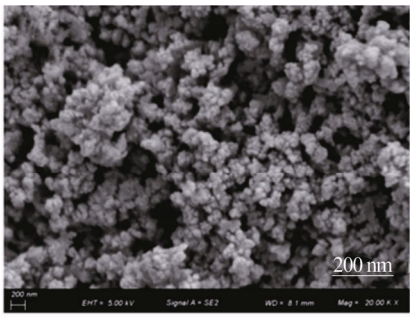

(c)

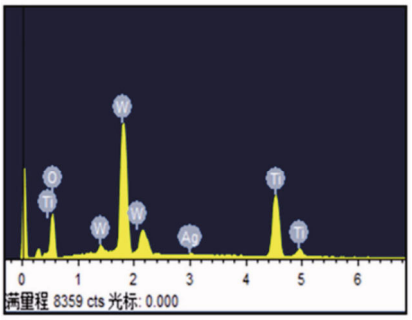

(d)

Fig.1 SEM images of (a) TiO_2, (b) TiO_2/WO_3, and (c) $Ag/TiO_2/WO_3$; (d) EDS spectra of $Ag/TiO_2/WO_3$ composite catalyst samples

The crystal phases of TiO_2, TiO_2/WO_3 and $Ag/TiO_2/WO_3$ are characterized by XRD (Fig.2(a)). The strong diffraction peaks at 2θ=23.6°, 24.37°, 33.6°, 34.1° and 41.9° can be indexed to the (020), (200), (222), (−202) and (202) of WO_3 (JCPDS 00-032-1395), respectively. The diffraction peaks at 2θ=24.37°, 42.1°, 48.5°, 54.0° and 62.7° are corresponding to (200), (101), (103), (200), (105) and (213) of TiO_2 (JCPDS 00-001-0562), respectively. The peaks near 2θ=38.8°, 44.1°, 64.7° and 78.3° can be indexed to (111), (200), (220) and (311) of Ag (JCPDS 00-003-0931), indicating that Ag was successfully mixed into the as-prepared samples.

In order to explore the absorption capacity of $Ag/TiO_2/WO_3$ composite nanostructures for sunlight, the UV-Vis diffuse reflectance spectroscopy (DRS) is carried out. It can be seen from Fig.3 that the absorption capacities of 406 nm, 459 nm, 486 nm and 502 nm correspond to TiO_2, WO_3, TiO_2/WO_3 and $Ag/TiO_2/WO_3$, respectively. The influence of band gap width on photocatalytic reaction is extremely important. The band gap width of the $Ag/TiO_2/WO_3$ composite sample is about 2.21 eV, which is less than 2.29 eV and 3.12 eV of TiO_2/WO_3 and pure TiO_2, respectively. The decrease of the band gap width indicates that abundant oxygen vacancies are generated on the surface of the $Ag/TiO_2/WO_3$ composite[16], thus decreasing the band gap and improving of photocatalytic activity of the materials.

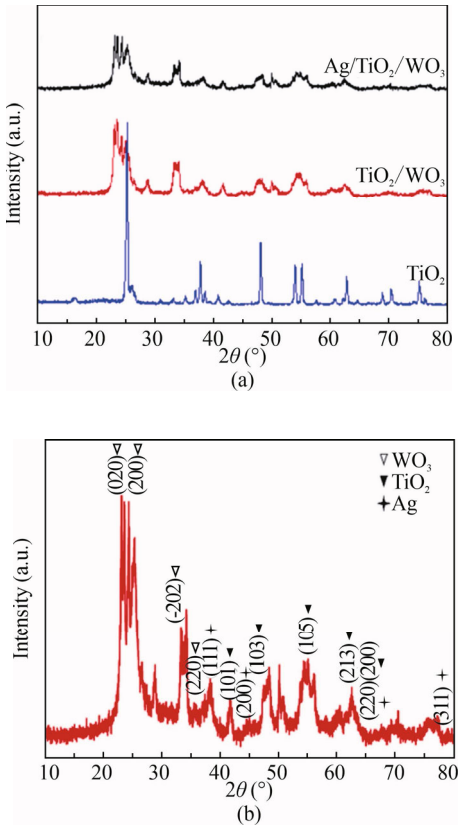

Fig.2 (a) XRD patterns of TiO_2, TiO_2/WO_3 and $Ag/TiO_2/WO_3$; (b) XRD magnified image of $Ag/TiO_2/WO_3$ sample

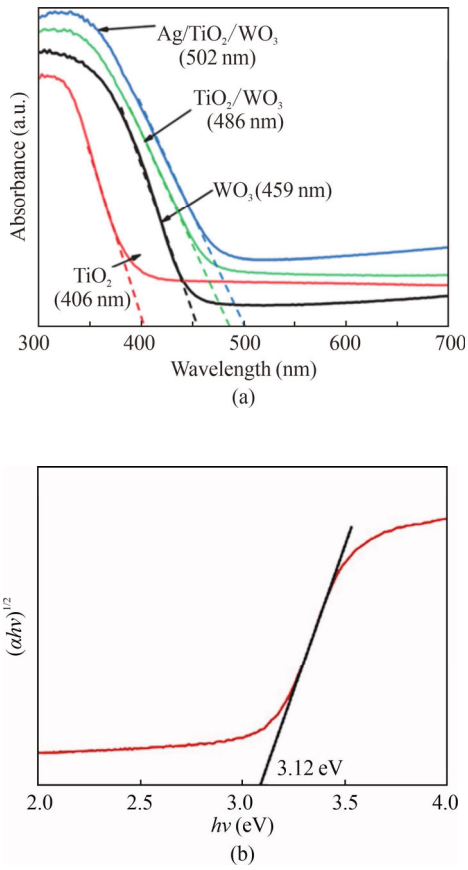

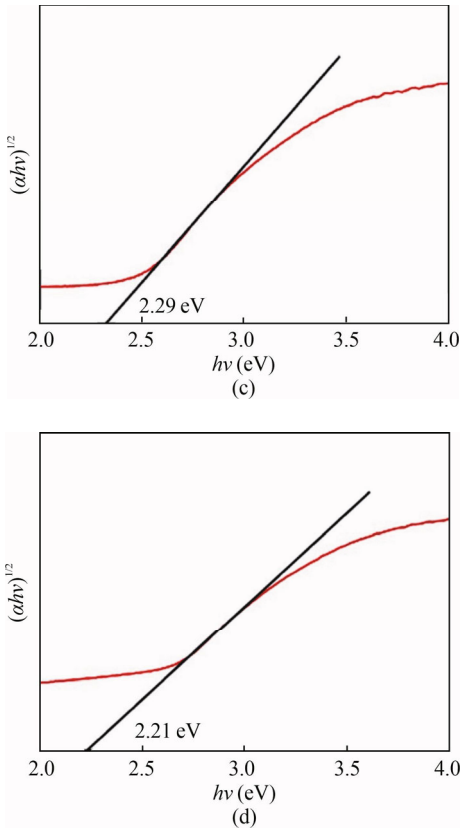

Fig.3 (a) UV-Vis DRS of TiO_2, TiO_2/WO_3 and $Ag/TiO_2/WO_3$ samples; The $(\alpha h\nu)^{1/2}$-$h\nu$ curves of (b) TiO_2, (c) TiO_2/WO_3, and (d) $Ag/TiO_2/WO_3$ samples

Fig.4 shows the EIS Nyquist plot of TiO_2, TiO_2/WO_3 and $Ag/TiO_2/WO_3$, respectively. It shows that the four samples follow the EIS radius trend of TiO_2>WO_3>TiO_2/WO_3>$Ag/TiO_2/WO_3$, which indicates that $Ag/TiO_2/WO_3$ catalyst with the best separation of photogenerated electron-hole pairs and the fastest charge mobility. It further illustrates that the electrochemical properties of the $Ag/TiO_2/WO_3$ composite are enhanced by combining TiO_2/WO_3 with Ag.

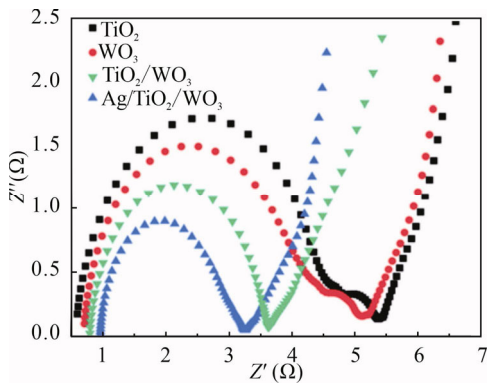

Fig.4 EIS Nyquist plotting of TiO_2, TiO_2/WO_3 and $Ag/TiO_2/WO_3$ samples

Fig.5(a) shows photoactalytic activity of as-prepared samples. It can be observed that $Ag/TiO_2/WO_3$ possesses

the photocaltalytic degradation rate of 96% within 20 min, which is higher than that of TiO_2/WO_3 (84%) and TiO_2 (6%) at the same conditions. The photocatalytic degradation results are consistent with those of UV-Vis DRS and EIS. The stability of photocatalyst is very important in practical application. Fig.5(b) shows that the $Ag/TiO_2/WO_3$ photocatalyst can still reach the degradation rate of 90% in the fifth degradation experiment, indicating a good stability and photocatalytic activity.

A possible mechanism of the enhanced photocatalytic degradation of $Ag/TiO_2/WO_3$ is proposed. When TiO_2 contacts with WO_3, the electrons (e^-) transfer from the conduction band of TiO_2 to WO_3 under UV-Vis light irradiation, while photogenerated holes (h^+) move from WO_3 towards TiO_2 in the valence band. Photogenerated e^- generates superoxide anions with the surrounding oxygen molecules, and photogenerated h^+ migrates to the surface of the heterojunction catalyst and reacts with water molecules to generate hydroxyl radicals. Superoxide anions and hydroxyl radicals eventually degrade pollutants into H_2O and CO_2 due to their strong oxidizing and reducing properties. The heterojunction can effectively improve the separation efficiency of photogenerated carriers and broaden the spectral absorption range of photocatalytic materials. When Ag particles is adsorbed on interface of the TiO_2/WO_3, the e^- will be captured by Ag in the combination of Ag and TiO_2/WO_3 interface to form a schottky barrier because the work function of Ag (4.26 eV) is generally higher than WO_3 (0.74 eV) and TiO_2 (−0.29 eV). The barrier can make the electron rich in the region of Ag particles, further promoting the separation of electrons-holes and enhancing the photocatalytic efficiency.

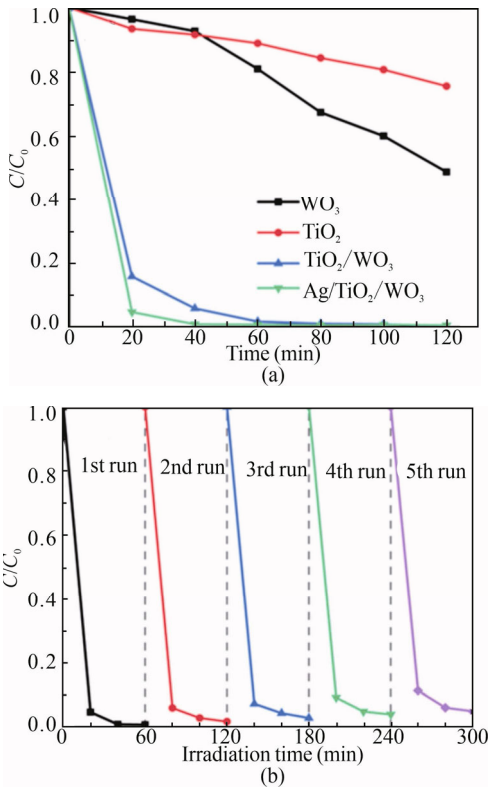

Fig.5 (a) Photocatalytic degradation curves to MB solution by four catalysts; (b) $Ag/TiO_2/WO_3$ composite catalyst cyclically degrading MB solution process

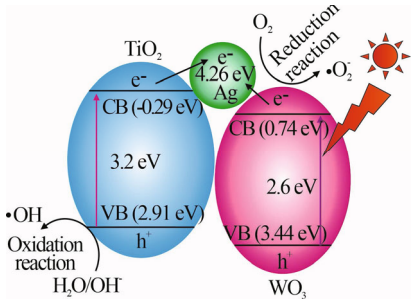

Fig.6 Photocatalytic mechanism of $Ag/TiO_2/WO_3$ composite catalyst

The distinctive $Ag/TiO_2/WO_3$ composite nanoparticles photocatalyst has been successfully synthesized by sol-gel method. The as-prepared Ag decorated TiO_2/WO_3 photocatalyst increases the specific surface area, enhances the visible light absorption, reduces current impedance and promotes the rate of electron-hole separation. As a result, $Ag/TiO_2/WO_3$ photocatalyst shows excellent photocatalytic performance. The photocatalytic efficiency of $Ag/TiO_2/WO_3$ photocatalyst achieves 96% in 20 min, which is 16 times higher than that of pristine TiO_2 at the same conditions. The $Ag/TiO_2/WO_3$ photocatalyst can still reach the degradation rate of 90% in the fifth degradation experiment, indicating that a good stability and photocatalytic activity.

Statements and Declarations

The authors declare that there are no conflicts of interest related to this article.

References

[1] YUAN C L, WANG Y Z, ZHU T, et al. Multistage biological contact oxidation for iandfill ieachate treatment： optimization and bacteria community analysis[J]. International biodeterioration & biodegradation, 2017, 125：200-207.

[2] BILINSKA L, GMUREK M, LEDAKOWICZ S. Comparison between industrial and simulated textile wastewater treatment by AOPs-biodegradability, toxicity and cost assessment[J]. Chemical engineering journal, 2016, 306：550-559.

[3] REVATHI J, ABEL M J, ARCHANA V, et al. Synthesis and characterization of $CoFe_2O_4$ and Ni-doped $CoFe_2O_4$ nanoparticles by chemical Co-precipitation technique for photo-degradation of organic dyestuffs under direct sunlight[J]. Physical B-condensed matter, 2020, 587：412136.

[4] FUJISHIMA A, HONDA K. Electrochemical photolysis of water at a semiconductor electrode[J]. Nature, 1972, 238：37-38.

[5] YUSUF Y, GHAZALI M J, OTSUKA Y, et al. Antibacterial properties of laser surface-textured TiO_2/ZnO ceramic coatings[J]. Ceramics international, 2020, 46(3)：3949-3959.

[6] WU T W, ZHU X J, XING Z, et al. Greatly improving electrochemical N-2 reduction over TiO_2 nanoparticles by iron doping[J]. Angewandte chemie-international edition, 2019, 58(51)：18449-18453.

[7] TERESCENCO D, HUCHER N, PICARD C, et al. Sensory perception of textural properties of cosmetic pickering emulsions[J]. International journal of cosmetic science, 2020, 42(2)：198-207.

[8] YU Q J, OUYANG T, ZHOU K F, et al. Photocatalytic degradation of oxytetracycline by photosensitive materials and toxicological analysis by caenorhabditis elegans[J]. Journal of nanoscience and nanotechnology, 2019, 19(11)：6924-6932.

[9] KARLSSON M, ABBAS Z, BOREDS R, et al. Characterisation of silicon, zirconium and aluminium coated titanium dioxide pigments recovered from paint waste[J]. Dyes and pigments, 2019, 162：145-152.

[10] CAI J M, WU M Q, WANG Y T, et al. Synergetic enhancement of light harvesting and charge separation over surface-disorder engineered TiO_2 photonic crystals[J]. Chemistry, 2017, 2(6)：877-892.

[11] WANG J, ZHANG Q, DENG F, et al. Rapid toxicity elimination of organic pollutants by the photocatalysis of environment-friendly and magnetically recoverable step-scheme $SnFe_2O_4$/$ZnFe_2O_4$ nano-heterojunctions[J]. Chemical engineering journal, 2020, 379：122264.

[12] WEI L J, ZHANG H M, CAO J. Electrospinning of Ag/$ZnWO_4$/WO_3 composite nanofibers with high visible light photocatalytic activity[J]. Materials letters, 2019, 236：171-174.

[13] WANG Q J, CUI Y, HUANG R J, et al. A heterogeneous Fenton reaction system of N-doped TiO_2 anchored on sepiolite activates peroxymonosulfate under visible light irradiation[J]. Chemical engineering journal, 2020, 383：123142.

[14] CHEN J, WANG M G, HAN J, et al. TiO_2 nanosheet/NiO nanorod hierarchical nanostructures：p-n heterojunctions towards effificient photocatalysis[J]. Journal of colloid and interface science, 2020, 562：313-321.

[15] YAO C L, CHENG L, ZHU J M. Synthesis, characterization and photocatalytic activity of Au/SiO_2@TiO_2 core-shell microspheres[J]. Journal of the Brazilian chemical society, 2020, 31：589-596.

[16] ZHAO Q H, FU L J, LIANG D H, et al. Nanoclay-modulated oxygen vacancies of metal oxide[J]. Communictions chemistry, 2019, 2：11.